J Mater Sci: Mater Med (2008) 19:1565–1573
DOI 10.1007/s10856-008-3400-y

In vivo behaviour of two different biphasic ceramic implanted in mandibular bone of dogs

Natalia Miño Fariña · Fernando Muñoz Guzón · Mónica López Peña · Antonio González Cantalapiedra

Received: 22 June 2007 / Accepted: 2 October 2007 / Published online: 26 February 2008

Abstract Alloplastic calcium phosphate bone substitutes such as hydroxyapatite (HA) and tricalcium phosphate (TCP) have been studied extensively due to their composition closely resembling the inorganic phase of bone tissue. On the same way, by manipulating the HA/TCP ratio it may be possible to change the substitution rate and the bioactivity of these materials, an advantage which has brought them to clinical use in oral and orthopaedic surgery. In this work, we evaluated the histological response in bone of two biphasic calcium phosphate ceramics by varying the proportion of their components. All premolars of 6 beagle dogs were removed from both sides of the mandible. Three months later, four cylinders composed of 85% HA and 15% β-TCP (BCP 1) were implanted in the right side of mandible and other four cylinders composed of 15% HA and 85% β-TCP (BCP 2) were implanted in the left side of mandible of dogs for 4, 12 ad 26 weeks, respectively. Two dogs were used in each time point. The histological study indicated that both biphasic ceramic were biocompatible. The earlier and more quantity of bone formed in BCP 2 than in BCP 1 suggested that the first one had a higher osteoinductive potential than the second one in mandibular bone. The resorption of the phosphate phase and the subsequent migration of bone into the resorbed portions were detected in both biphasic ceramics although two processes appeared faster in BCP 2 than in BCP 1. These dates conclude that varying the components of our biphasic ceramic we improve its osteoinductive potential.

N. M. Fariña (✉) · F. M. Guzón · M. L. Peña · A. G. Cantalapiedra
Departamento de Ciencias Clínicas Veterinarias, Universidad de Santiago de Compostela, Campus universitario, s/n, 27002 Lugo, Spain
e-mail: natmin@lugo.usc.es

1 Introduction

World-wide bone grafting is the second most frequent transplant procedure after blood transfusion. Autograft, allograft (including demineralized bone matrix), and synthetic materials (metals, polymers and ceramics) are the choices in clinics to repair bone in orthopaedic, spinal and craniomaxillofacial (dental) surgeries [1–6]. The limitations of autogenous grafts and allogeneic bankbone have led to a search for synthetic alloplast alternatives. Calcium phosphates bone substitutes such as hydroxypapatite (HA) and tricalcium phosphate (TCP) have been widely used because the mineral composition of these implants materials does fully biocompatible [7–10].

The porous structure of the ceramics is claimed to enhance bone deposition and implant stabilization in the recipient bone [11]. The optimal pore size is still debated to be ranging from 50 μm and 565 μm [12, 13]. However, porosity of the material is inversely proportional to the mechanical stability of these calcium phosphate-based ceramics [1]. This loss of stability is often cited as a limitation in the use of calcium phosphate-based ceramics in clinical practice. A convenient compromise to overcome this problem is to use a biphasic calcium phosphate ceramic that consists of a hydroxyapatite bioactive matrix (HA) and a dispersed phase of reabsorbable phosphate (β-TCP) [13, 14]. These materials maintain their mechanical resistance until the resorption is achieved. Therefore, it can provide good scaffold for the new bone to grow owing to HA, otherwise, it can have bioactivity for bone remodelling owing to β-TCP. In the same way, it is demonstrated that physicochemical modifications could improve the biological properties of the materials [2, 8, 15–17].

Aiming at clinical application, we evaluated the histological response in bone of two biphasic calcium phosphate ceramics by varying the proportion of their components.

Thereby, the influence of the HA/β-TCP ratio on new bone formation, graft degradation and bone-to-graft contact could be compared.

2 Material and methods

2.1 Biomaterial preparation

In this study, two BCP ceramics were used: BCP 1 and BCP 2. Both of them are made of hydroxiapatite (HA) and β-tricalcium phosphate (β-TCP), only varying the proportion of these two components:

- BCP 1: 85% HA and 15% β-TCP
- BCP 2: 15% HA and 85% β-TCP

BCP 1 and BCP 2 were prepared in a similar way. Firstly, apatite powders were prepared by precipitation method. For the production of HA, apatite powder was prepared with a Ca/P ratio of 1.67, at PH $>$ 11 and a temperature of 65°C. For β-TCP, apatite powder was prepared with Ca/P ratio of 1.5, at PH $>$ 10 and a temperature of 25°C. HA and β-TCP were sintered at 1,000°C for 1 h. Compositions and crystal structures of the ceramics were determined from X-ray diffraction (XRD) (Fig. 1a, b). After the characterization, BCP implants were prepared by mixing HA and β-TCP powders with a mean particle size of 5 μm in the required proportions. A lathe was used to produce BCP ceramic cylinders with a diameter of 2 mm and a length of a 6 mm (Fig. 2) and next they were dried and sintered at 1,100°C for 8 h.

All implants were cleaned in ultrasonic baths and sterilized by gamma radiation.

2.2 Biomaterial examination

Prior to implantation, composition and crystal structure of the ceramics were determined by using X-ray diffraction (XRD). From each type of ceramic, 0.5 g was ground into a fine powder in an agate mortar and loaded into a rotatable specimen holder. BCP 1 and BCP 2 powders were examined ($2° < 2\theta < 60°$) using a Philips PW1710 Kristalloflex diffractometer with 0.02° resolution. HA/β-TCP weight ratios in the BCP ceramics were calculated by comparing the BCP XRD patterns prepared from the powders with the known HA/β-TCP weight ratios.

Also, ultrastructure of both ceramics was characterized by a scanning electron microscopy (Leica, 440) in the secondary electron mode.

2.3 Surgical procedure

The study protocol was approved by the Regional Ethics Committee for Animal Research. Six beagle dogs, about 2 years old and 20 kg weight, were enrolled in the study. During surgical procedures, the animals were premedicated with acepromacine (0.05 mg/Kg intramuscularly) and morphine (0.2 mg/Kg intravenously). Immediately afterward, they were induced general anesthesia by injection of propofol (2 mg/Kg intravenously). Isofluorane (1.5–2%) and O_2 (100%) were used as inhalated anaesthetics.

All premolars were removed from both sides of the mandible in each dog and healing was allowed for 3 months. After this period, four cylinders composed of BCP 1 were implanted in the right side of mandible and other four cylinders composed of BCP 2 were implanted in the left side of mandible of dogs for 4, 12 ad 26 weeks, respectively. Two dogs were used in each time point.

The animals were euthanized with an overdose of sodium pentobarbital through the cephalic veins.

2.4 Histological preparation

The mandibles were removed and block biopsies of each implant were dissected using an oscillating saw. The samples were fixed 1 week in 10% formol. Next, the samples were dehydrated in different graded ethanol series (70–100%), and infiltrated with 4 different graded mixtures of ethanol and infiltrating resine, glicometacrilate (Technovit 7200®, VLC—Heraus Kulzer GMBH) with 1% of Benzoyle Peroxide (BPO®: Heraus Kulzer GMBH). The last infiltration was performed with pure infiltrating resine under vacuum. The samples were then polymerized, first under low intensity UV light for 4 h, followed by a polymerization under high intensity UV light for 12 h and finally by keeping the samples heated for 24 h to assure complete polymerization.

The samples were glued to a sample holder. Longitudinal sections of 200 μm were cut with a band saw (Exakt 400, System, Aparatebau GMBH), and were polished with 1,200 and 4,000 silicon carbide papers (Exakt-Micro Griding System®) until a samples thickness of 70 μm was obtained and all sections were stained with Lévai Laczkó stain for both histological examination and histomorphometric analysis.

2.5 Histomorphometric analysis

Histomorphometry was performed on the sections taken to determine the bone regeneration and the bone contact using a current optical microscope (Olympus CH30) with a digital camera attached (Olympus DP12) and a computer-based image analysis system (MicroImage 1.0). Briefly, the percentages of bone contact (the length of bone directly opposed to the implant without the presence of a fibrous membrane/the total length of the bone-implant interface multiplied by 100) and bone formation around the implant

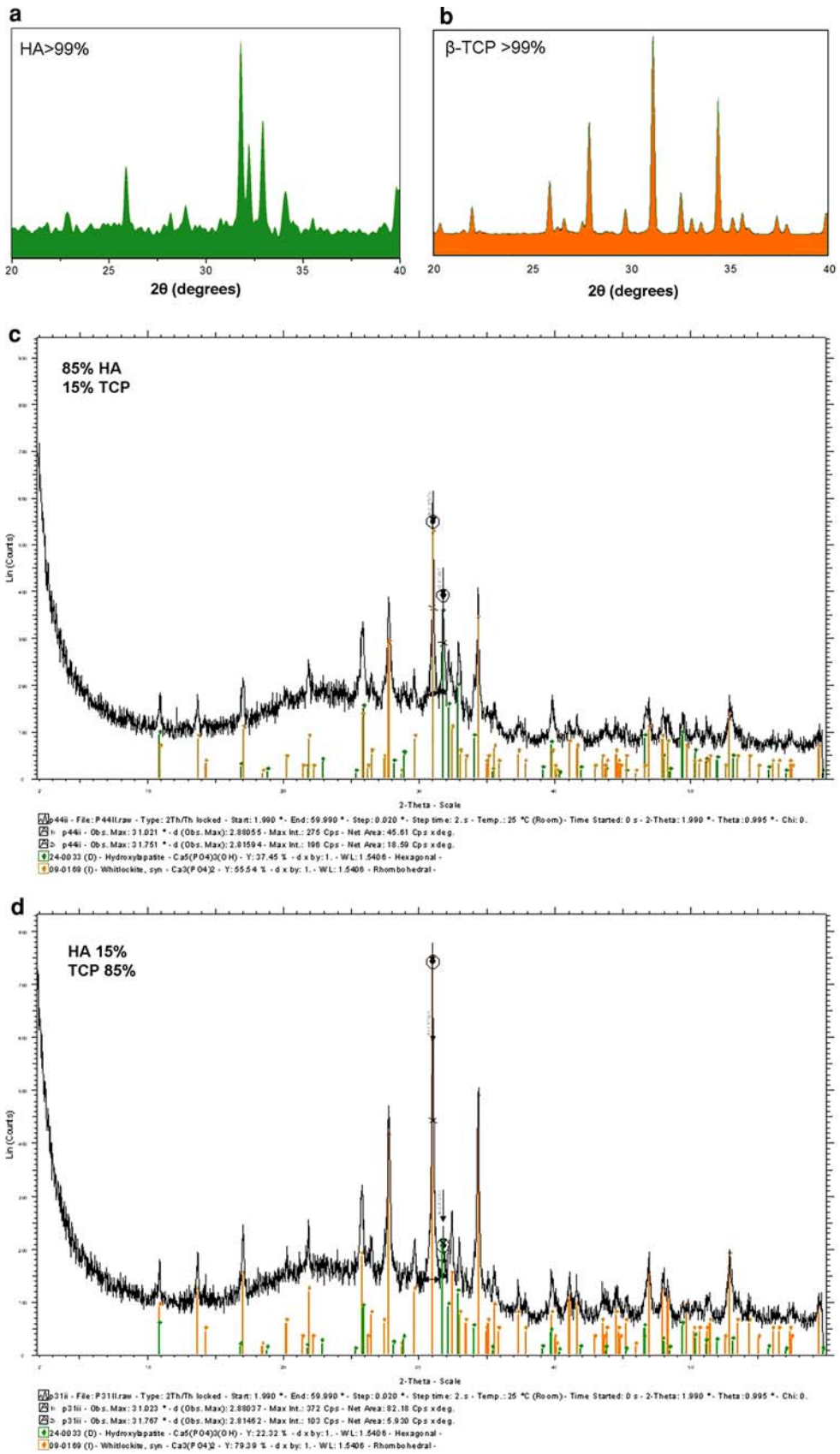

Fig. 1 Physicochemical characterization of samples from HA (**a**), β-TCP (**b**), BCP 1 (**c**) and BCP 2 (**d**). Green patterns denote hydroxyapatite and green patterns denote tricalcium phosphate

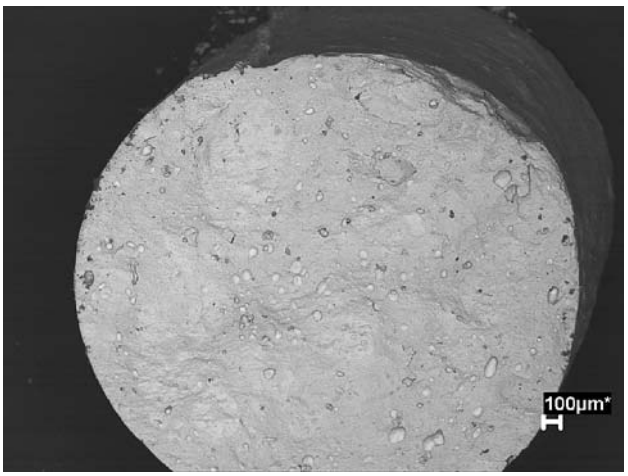

Fig. 2 SEM imaging of a cylinder of BCP 1 (original magnification 95×)

(the bone area in 1 mm around the implant/the total area in 1 mm around the implant multiplied by 100) were semi-automatically measured by a blinder investigator at a magnification of 40×.

2.6 Scanning electron microscopy (SEM)

The PMMA embedded specimens obtained from the histological preparation were mounted on a scanning electron microscope (LEO−435 VP) with beam voltages of 0.3–30 kV. Quantification for calcium (Ca), phosphorus (P) and magnesium (Mg) was determined by X-ray microanalysis by an energy dispersive X-ray detector attached to the SEM and performed at four regions (0.05 × 0.05 mm): the central region of the implant (A), the region within the implant adjacent to the interface between the implant and bone (B), the region within the bone adjacent to the interface (C) and the bone (D). Within each region, measurements were made at three points and the averages were calculated.

The quantity of resorbed ceramic was determined using the computer-based image analysis system (MicroImage 1.0) from SEM observations of implant surfaces obtained with the secondary electron mode (LEO−435 VP). The total implant surface area was divided into 12 adjacent fields and recorded on SEM (magnification 95×). The threshold was determined by the operator on the image analyzer, and the three surface tissue components (ceramic, soft tissues and newly formed bone) were identified using artificial colours. Their respective areas were automatically calculated by a blinder investigator and expressed as a percentage of the total surface area. The degradation rate was calculated as the difference between the BCP percentage before and after implantation.

2.7 Statistical analysis

The statistical analysis was carried out on the quantitative data from histological sections and implant surface data from BSE images using SPSS 12.0 software for windows. Data are reported as mean ± SD at a significance level of $P < 0.05$. The one way analysis of variance followed by an a posteriori Tukey test across the time was chosen.

3 Results

3.1 Surgeries

All surgeries went well with no clinical evidence of inflammatory response to the ceramic implant and no toxic signs during the experimental period.

3.2 Material characterization

XRD patterns of the two BCP ceramic are given in Fig. 1c, d. Both BCP ceramics had similar, biphasic structure, consisting of HA and β-TCP. However, HA/β-TCP weight ratio differed: BCP 1 ceramic consisted of 85 ± 5 wt% HA and 15 ± 5 wt% β-TCP, while contents of HA and β-TCP in BCP 2 were 15 ± 5 wt% and 85 ± 5 wt%, respectively, which is illustrated by the differences in the height of the main β-TCP peak (at $2\theta = 31.2°$) in the BCP XRD patterns.

Microstructures of the ceramics were very similar, as illustrated by Figs. 3 and 4.

3.3 SEM study

In SEM images, newly formed bone appeared to be qualitatively similar for both BCP ceramics, regardless of the implantation period (Figs. 5 and 6).

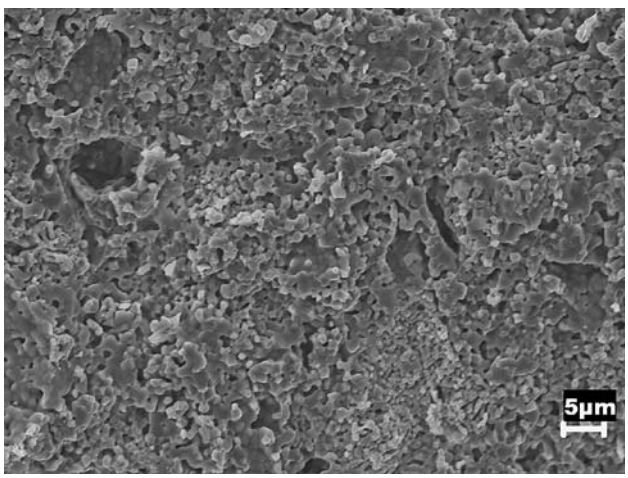

Fig. 3 SEM imaging of BCP 1 (original magnification 5,000×)

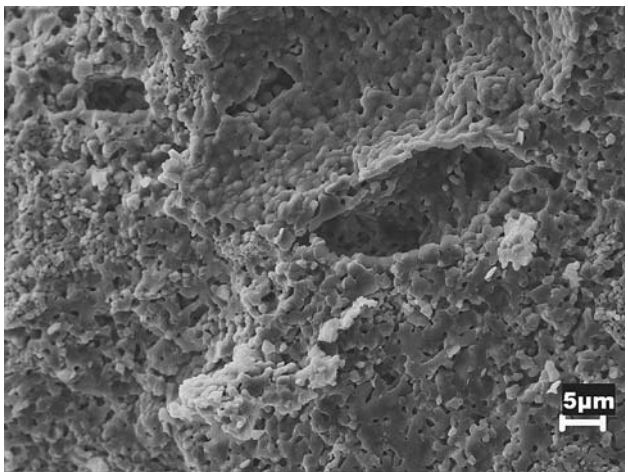

Fig. 4 SEM imaging of BCP 2 (original magnification 5,000×)

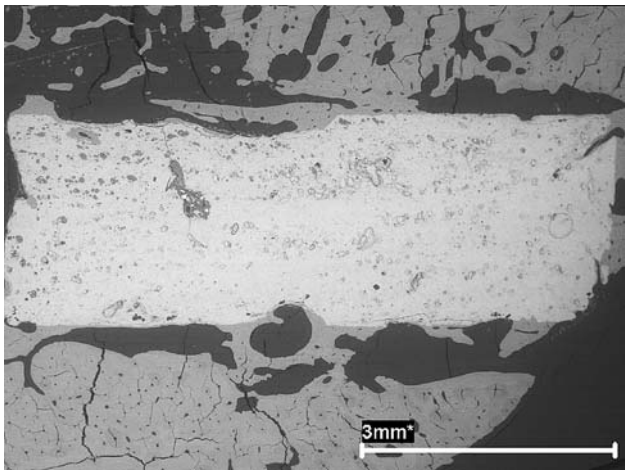

Fig. 5 SEM imaging of BCP 1 at 26 weeks after implantation (original magnification 50×)

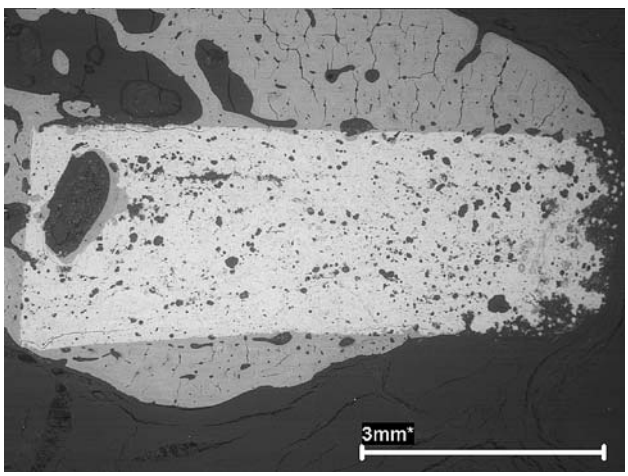

Fig. 6 SEM imaging of BCP 2 at 26 weeks after implantation (original magnification 50×)

Table 1 Quantification for biodegradation determined from BSE images

Implant	Biodegradation rate (%)		
	Time periods		
	4	12	26
BCP 1 ($N = 8$)	2.01 (±1.05)	2.3 (±1.56)	4.25 (±1.95)
BCP 2 ($N = 8$)	4.03 (±1.53)	5.6 (±2.03)	12.49 (±2.66)*

* Significantly higher than biodegradation on the BCP 1 at 26 weeks ($P < 0.05$)

Analysis of implant surfaces from SEM images indicated that all implants were partially degraded and the statistical study showed that the degradation rate was significantly greater for BCP 2 implants than for BCP 1 implants at 26 weeks ($P < 0.05$) (Table 1).

3.4 X-ray microanalysis

Quantitative elemental analysis data are summarized in Table 2. The results obtained revealed that the ratio of calcium to phosphorus at the central region (A) and surface (B) of the BCP 1 was slightly higher than BCP 2 and bone. A small quantity of magnesium, which was not contained in the BCP powders, was detected in the central region in a quantity about one-fourth as much as the quantity at the peripheral region.

3.5 Histological study

In all specimens, no signs of inflammation were detectable either macroscopically or microscopically.

Histological views of BCP 1 and BCP 2 implanted in mandibular bone of dogs at 4, 12 and 26 weeks are shown in Fig. 7 (magnification 100×). Close observation of bone formation (magnification 400×) showed that blood vessels and osteoid secreted by osteoblast-like cells were observed surrounding all the implants (Fig. 8a) at 4 weeks. Bone formation was mainly confined to the edges of the defect in BCP 1 (Fig. 8a), but in BCP 2 it was mostly detected on the implant surface (Fig. 8b). At 12 weeks, clear osteoblast line, newly formed bone matrix, osteocytes, and mineralized bone were observed on the outer surface of BCP 1 implant and host bone bed (Fig. 8c). Bone remodelling was observed as indicated by the osteoclast-like cells lining in the resorbed portions close to the host bone bed in BCP 2 and host bone bed (Fig. 8d). At 26 weeks, the early formed bone became mature bone with harversian's canals in both implants (Fig. 8e, f). Resorption of implants was hardly observed in both BCP ceramics at any time point.

Table 2 Quantification for Ca, P and Mg determined from EDX

	BCP 1 ($N = 8$)				BCP 2 ($N = 8$)			
	A	B	C	D	A	B	C	D
4 weeks								
Ca/P	1.626 (±0.03)	1.625 (±0.03)	1.570 (±0.02)	1.558 (±0.05)	1.521 (±0.03	1.523 (±0.05)	1.557 (±0.03)	1.557 (±0.04)
Mg (%)	0.054 (±0.02)	0.065 (±0.01)	0.184 (±0.01)	0.198 (±0.02)	0.062 (±0.01)	0.063 (±0.01)	0.201 (±0.02)	0.198 (±0.03)
12 weeks								
Ca/P	1.618 (±0.05)	1.611 (±0.04)	1.557 (±0.03)	1.558 (±0.07)	1.535 (±0.06)	1.5390 (±0.05)	1.556 (±0.04)	1.557 (±0.06)
Mg (%)	0.050 (±0.01)	0.062 (±0.02)	0.195 (±0.01)	0.188 (±0.02)	0.071 (±0.01)	0.070 (±0.01)	0.204 (±0.02)	0.198 (±0.03)
26 weeks								
Ca/P	1.613 (±0.05)	1.606 (±0.04)	1.560 (±0.03)	1.561 (±0.07)	1.551 (±0.05)	1.556 (±0.04)	1.558 (±0.06)	1.560 (±0.07)
Mg (%)	0.055 (±0.01)	0.068 (±0.02)	0.178 (±0.01)	0.198 (±0.03)	0.056 (±0.01)	0.067 (±0.03)	0.181 (±0.02)	0.188 (±0.03)

A—central region in the BCPs; B—region adjacent to interface within the implants; C—region adjacent to interface within bone; D—bony region

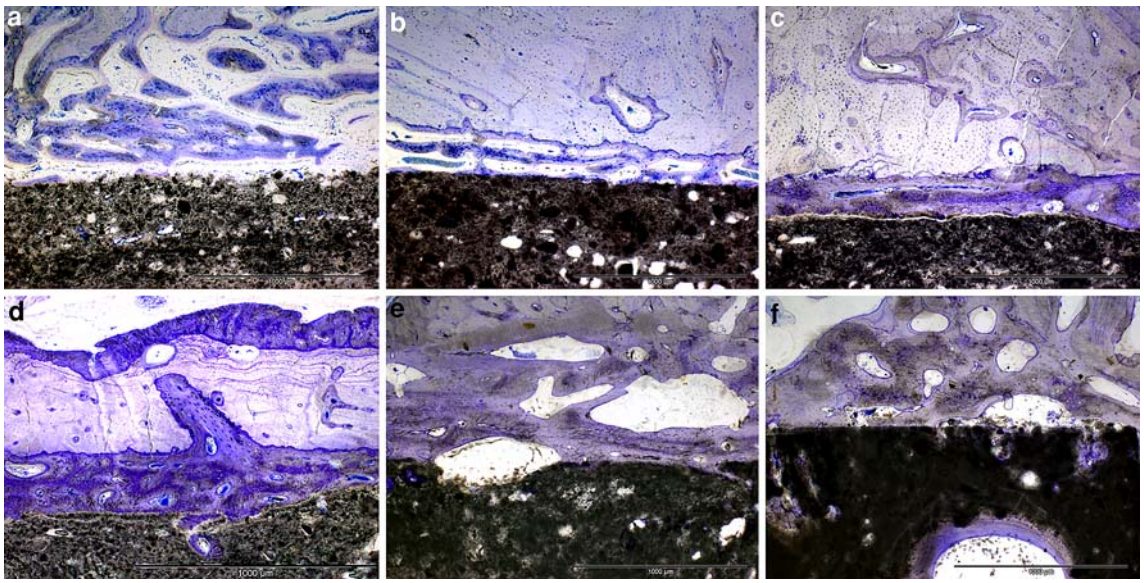

Fig. 7 Histological overviews of bone formation in BCP ceramics implanted in mandibular bone of dogs: (**a**) BCP 1, 4 weeks; (**b**) BCP 2, 4 weeks; (**c**) BCP 1, 12 weeks; (**d**) BCP 2, 12 weeks; (**e**) BCP 1, 26 weeks; (**f**) BCP 2, 26 weeks. Decalcified section stained with Lévai Laczkó staining

The processes of bone formation in BCP 1 and BCP 2 implanted in mandible of dogs, including cell attachment on BCP surface, cell proliferation and differentiation on BCP surface, formation of bone matrix by osteoblast-like cells on BCP surface, mineralization of bone matrix on BCP surface, bone remodelling, bone marrow formation, and formation of mature bone were similar, but each step took place earlier in BCP 2 than in BCP 1.

3.6 Histomorphometric analysis

Quantitative data of bone formation and bone contact are summarized in Table 3. It showed significant change in the percentage of bone contact of BCP 1 at 26 weeks and in the percentage of bone contact of the BCP 2 at 12 weeks. The percentage of bone formation of both ceramics was significantly higher at 26 weeks postoperatively. The

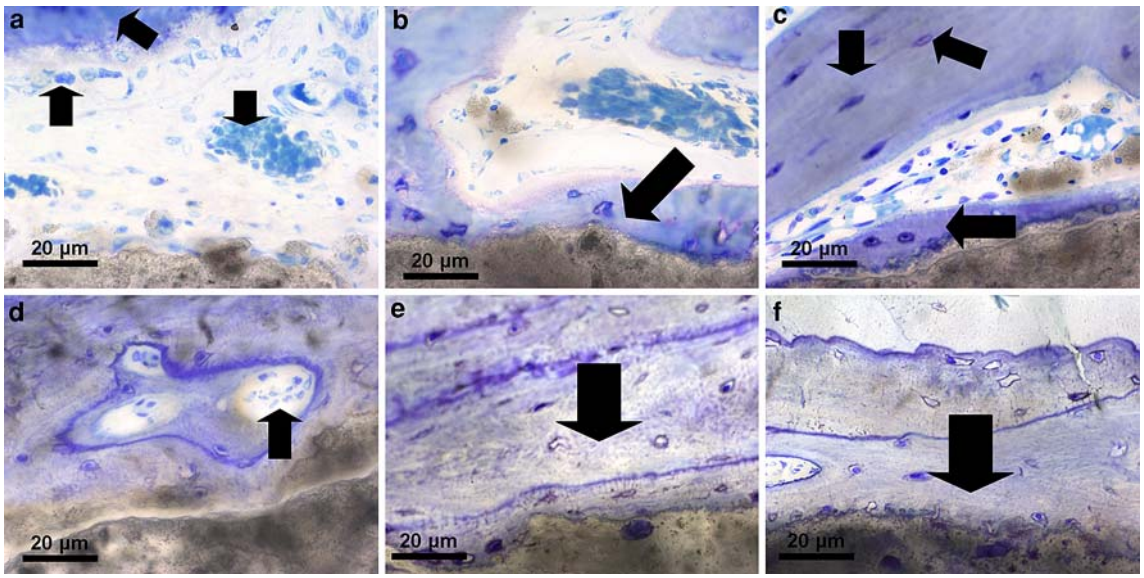

Fig. 8 Tissue responses to BCP ceramics after mandibular bone implantation in dogs for different time periods: (**a**) BCP 1, 4 weeks: Blood vessels (⬇) and osteoid (⬉) secreted by osteoblast (⬆) confined to the edges of the defect; (**b**) BCP 2, 4 weeks: Bone formation detected on the implant surface (⬋); (**c**) BCP 1, 12 weeks: newly formed bone matrix (⬅), osteocytes (⬉), and mineralized bone (⬇) observed on the outer surface implant and host bone bed; (**d**) BCP 2, 12 weeks: Bone remodelling observed in the macropores close to the host bone bed as indicated by the osteoclast-like cells lining (⬆); (**e**) BCP 1, 26 weeks: mature bone with harvesian's canals (⬇) and (**f**) BCP 2, 26 weeks: mature bone with harversian's canals (⬇). Decalcified section stained with Lévai Laczkó staining

Table 3 Quantification for bone contact and bone formation determined from histomorphometric analysis

Implant	% bone contact			% bone formation		
	Time periods (w)			Time periods (w)		
	4	12	26	4	12	26
BCP 1 ($N = 8$)	27.4 (±2.85)	64.1 (±4.42)	72.8* (±5.14)	42.3 (±3.75)	60.7 (±5.62)	81.7* (±7.12)
BCP 2 ($N = 8$)	58.9** (±3.69)	65.0* (±4.14)	83.3 (±5.52)	57.0 (±4.52)	67.3 (±5.24)	87.3* (±6.13)

* Significantly different from bone contact of 12 weeks (BCP 2) and 26 weeks (BCP 1) and bone formation of 26 weeks (BCP 1 and BCP 2) ($P < 0.05$)

** Significantly higher than bone contact on the BCP 1 at 4 weeks ($P < 0.05$)

percentage of bone contact of BCP 2 was significantly higher at 4 weeks compared to that on BCP 1.

4 Discussion

The ability of an osteopromotive material to enhance bone regeneration and generate osseous union when implanted in the experimental defect should always be tested in an experimentally created bone defect, which has been tested previously to fulfil the standards of a critical-size bone defect [1, 11, 18]. Therefore, we have used the critical size defects in our experimental study.

In our experiment, BCP ceramics with a block form have been studied. Merx et al. have demonstrated that a block form has the advantage that is more efficient than the particular form and new bone apposition happens with progressive material degradation [18–20]. On the other hand, Yuan et al. reported that particular BCP might present the advantage to be more easily combined with cultured osteogenic cells or loaded growth factors, which are promising ways for bone repair [21]. Calcium phosphate particles have also the advantage to be easier to handle than block form, that has to be shaped the exact form of the defect, but generally when granules are used in osteo-articular surgery, some grains will be released in cartilage or non osseous site [22, 23].

This work compared the biological behaviour of two BCP ceramics that differed significantly in their composition. Both BCP ceramics induced bone formation in mandible of dogs, while BCP 2 induced an earlier bone formation and more bone than BCP 1. Meanwhile, BCP 2 got faster bone formation than BCP 1. It seems that the superiority of BCP 2 is not really due to greater bone ingrowth but to its capacity to undergo early and intense bone substitution in early implantation times, as confirmed in the histomorphometric analysis. This capacity suggests that BCP 2 is more favourable than BCP 1 for cellular

events as well as consecutive ceramic resorption—bone formation [8, 24].

Having a high TCP content, mainly BCP 2, both ceramics could be expected to be proportionally resorbed at a longer implantation time as it was observed by other authors [25], but at 26 weeks we only observed a degradation rate of 12,49% (±2.66) in BCP 2 and 4.25% (±1,95) in BCP 1. In this way, Yuan et al. have also detailed previously that no clear resorption of BCP ceramics regarding the decrease of implant size was observed in their study [2]. These authors suggested that one reason might be the method form which their BCP had been prepared. Another reason that they proposed was related to the formation of bone on the material surface. Since chemical dissolution and cell-mediated resorption were demonstrated to be involved in material resorption in vivo, the formed bone on BCP surface would have slowed the chemical dissolution and decreased the material surface area that multinucleated cells or osteoclast could reach. As a result, BCP could only be resorbed during bone remodelling at a low speed. Gauthier et al. have also found that their BCP particles were not completely degraded after long-term (78 weeks) implantation [8]. In this study, ultrastructural analysis indicated that HA was the remaining calcium phosphate phase. This suggests that BCP ceramics can associate sufficient bioactivity and biodegradability with adequate in vivo stability to allow extensive and viable substitution [8, 9].

Our study also showed in SEM images that BCP 2 exhibited a higher degradation rate during the study than BCP 1 due to the HA/β-TCP ratio: the lower the ratio, the higher the extent of dissolution [27]. This data showed that, although both ceramics had presented similar specific surface area before implantation, the size of the resorbed portions created during the study was directly related to osteoinductive properties: the longer the resorbed portions the higher bone formation [17, 21]. In this sense, Habibovic et al. found that the difference related to the macrostructure of two BCP ceramics could improve their osteoinductive properties [15]. As recently reviewed by Karageorgiu and Kaplan, based on early studies, the minimum requirement for pore size is considered to be ±100 μm because of cell size, migration requirements, and nutrient transport. However, pore sizes higher than 300 μm are recommended because of the formation of capillaries [25]. For this reason, it is possible that the larger areas of resorbed ceramic that appeared in BCP 2 in comparison with BCP 1 were responsible for better nutrient and cell distribution and capillary formation.

In addition to the macrostructure, the dissolution of calcium phosphate materials would have added values to the higher osteoinductive potential of BCP 2 as well. It is known that TCP has a higher dissolution rate than HA; meanwhile, calcium and phosphate can promote

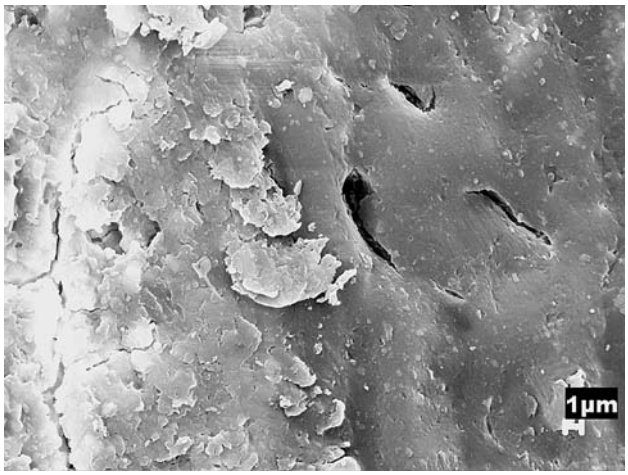

Fig. 9 SEM imaging showing the formation of carbonate hydroxiapatite on surfaces of BCP 2 crystals 26 weeks after implantation. It also shows bone growth closely associated to the ceramic (original magnification 10,000×)

mineralization of bone cells at specific concentrations [26–28]. Since BCP 2 contained more β-TCP than BCP 1, higher local calcium phosphate concentrations could have had a stimulatory effect on bone matrix mineralization in BCP 2 implants (Fig. 9). On this way, Daculsi et al. observed the formation of mycrocrystals with Ca/P ratios similar to those of bone apatite crystals after the implantation by diffraction X-rays [29]. The abundance of those crystals was directly related to the initial HA/β-TCP ratio in the BCP: the higher the ratio the greater the abundance of the mycrocrystals associated with the BCP crystals.

5 Conclusions

The histological study indicates that both biphasic ceramic are biocompatible. The earlier and more quantity of bone formed in BCP 2 than in BCP 1 suggests the first one has a higher osteoinductive potential than the second one in mandibular bone. The resorption of the phosphate phase and the subsequent migration of bone into the resorbed portions were detected in both biphasic ceramics although two processes appear faster in BCP 2 than in BCP 1. These data show that the variation in HA/β-TCP ratio was suitable to improve bone formation. Considering these results, we demonstrate that by introducing into synthetic materials, such as BCP ceramics of our study, the factors having positive influence on cell attachment, cell proliferation and differentiation, bone mineralization and bone remodelling, would be potential ways to further optimize synthetic materials into highly osteoinductive materials, which could induce bone formation as early as possible and as much as possible.

Acknowledgements The authors thank the Spanish Ministry of Education for funding this work through CICYT project MAT2002-00815.

References

1. H. Develioglu, S.Ü. Saraydin, L. Dupoirieux, Z.D. Sahin, J. Biomed. Mater. Res. A **80**, 505 (2007)
2. H. Yuan, C.A. Van Blitterswijk, K. De Groot, J.D. De Brujin, J. Biomed. Mater. Res. A **78**, 139 (2006)
3. R.R. Betz, Orthopedics. **25**, 561 (2002)
4. S.N. Parik, J. Postgrad. Med. **48**, 142 (2002)
5. S.N. Khan, E. Tomin, J.M. Lane, Orthop. Clin. North Am. **31**, 389 (2000)
6. H. Yuan, K. Kurashina, J.D. De Brujin, Y. Li, K. De Groot, X. Zhang, Biomaterials **20**, 1799 (1999)
7. M. Vallet-Regí, J. Chem. Soc., Dalton Trans. **2**, 97 (2001)
8. O. Gauthier, E. Goyenvalle, J.-M. Bouler, J. Guicheux, P. Pilet, P. Weiss, G. Daculsi, J. Mat. Sci. Mat. Med. **12**, 385 (2001)
9. G. Daculsi, Biomaterials **19**, 1473 (1998)
10. L.L. Hench, J. Am. Ceram. Soc. **74**, 1487 (1991)
11. H. Develioglu, S.Ü. Saraydin, G. Bolayir, L. Dupoirieux, J. Biomed. Mater. Res. A **77**, 627 (2006)
12. B.S. Chang, C.K. Lee, K.S. Hong, H.J. Youn, H.S. Ryu, S.S. Chung, K.W. Park, Biomaterials **21**, 1291 (2000)
13. O. Gauthier, J.M. Bouler, E. Aguado, P. Pilet, G Daculsi, Biomaterials **19**, 133 (1998)
14. G. Daculsi, R.Z. Geros, E. Nery, K. Lynch, B. Kerebel, J. Biomed. Mater. Res. **23**, 883 (1989)
15. P. Habibovic, T.M. Sees, M.A. Van Den Doel, C.A. Van Blitterswijk, K. De Groot, J. Biomed. Mater. Res. A **77**, 747 (2006)
16. P. Habibovic, H. Yuan, C.M. Van Der Valk, G. Meijer, C.A. Van Blitterswik, K. De Groot, Biomaterials **26**, 3565 (2005)
17. H. Yuan, J.D. De Bruijn, Y. Li, J. Feng, Z. Yang, K. De Groot, X. Zhang, J. Mat. Sci. Mat. Med. **12**, 7 (2001)
18. M.A. Merkx, J.C. Maltha, H.P. Freihofer, A.M. Kujpers-Jagtman, Biomaterials **20**, 2029 (1999)
19. G. Daculsi, R.Z. Legeros, M. Heughebaert, I. Barbieux, Calcif. Tissue Int. **46**, 20 (1990)
20. G. Daculsi, N. Passuti, Biomaterials **11**, 86 (1990)
21. H. Yuan, M. Van Den Doel, S. Li, C.A. Van Blitterswijk, K. De Groot, J.D. De Bruijn, J. Mat. Sci. Mat. Med. **13**, 1271 (2002)
22. D.J. Bell, J. Prosthet. Dent. **56**, 322 (1986)
23. M.S. Block, J.N. Kent, J. Oral Maxillofac. Surg. **44**, 44 (1986)
24. P. Habibovic, H. Yuan, M. Van Den Doel, T.M. Sees, C.A. Van Blitterswijk, K. De Groot, J. Orthop. Res. **24**, 867 (2006)
25. C. Schopper, F. Ziya-Ghazvini, W. Goriwoda, D. Moser, F. Wanschitz, E. Spassova, G. Lagogiannis, A. Auterith, R. Ewers, J. Biomed. Mater. Res. A **4**, 458 (2005)
26. V. Karageorgiu, D. Kaplan, Biomaterials **26**, 5474 (2005)
27. R.Z. Legeros, S. Lin, R. Rohanizadeh, D. Mijares, J.P. Legeros, J. Mat. Sci. Mat. Med. **14**, 201 (2003)
28. Y.-L. Chang, C.M. Stanford, J.C. Keller, J. Biomed. Mater. Res. **52**, 270 (2000)
29. G. Daculsi, O. Laboux, O. Malard, P. Weiss, J. Mat. Sci. Mat. Med. **14**, 195 (2003)